Astragaloside IV Reduces Mutant Ataxin-3 Levels and Supports Mitochondrial Function in Spinocerebellar Ataxia Type 3

Yongshiou Lin
Changhua Christian Hospital
Wenling Cheng
Changhua Christian Hospital
Juichih Chang
Changhua Christian Hospital
Yuling Wu
Buddhist Tzu Chi General Hospital Hualien: Hualien Tzu Chi Hospital
Mingli Hsieh
Tunghai University
Chin-San Liu (liu48111@gmail.com)
Changhua Christian Hospital https://orcid.org/0000-0001-8241-9654

Research Article

Keywords: spinocerebellar ataxia type 3, astragaloside IV, oxidative stress, autophagy, mitochondrial dysfunction, antioxidant capacity

Posted Date: September 20th, 2023

DOI: https://doi.org/10.21203/rs.3.rs-3350835/v1

Abstract

This study investigated the effects of astragaloside IV (AST) on the neurodegenerative disease of spinocerebellar ataxia type 3 (SCA3). Human neuroblastoma SK-N-SH cells expressing mutant ataxin-3 protein with 78 CAG repeats (MJD78) were used as an in vitro model, and SCA3 transgenic mice harboring an allele with a pathological polyglutamine tract with expanded 84 CAG repeats (SCA3 84Q) were used as an in vivo model. Protein expression analysis revealed that AST treatment reduced mutant ataxin-3 protein expression and aggregation via increased the autophagic flux in the MJD78 cells. Oxidative stress levels were elevated in the MJD78 cells but were reduced after AST treatment, which also increased antioxidant capacity; these findings were obtained using flow cytometry and antioxidant enzyme activity assay. Furthermore, treatment with AST ameliorated mitochondrial dysfunction in the MJD78 cells, including that related to mitochondrial membrane potential, respiration, and mitochondrial dynamics. Additionally, AST administration improved motor function and provided protection against Purkinje cell loss in the cerebellum of the SCA3 84Q mice.

In conclusion, AST administration increase the capability of antioxidants and reduced either cellular or mitochondrial oxidative stress and improve the process of mitochondrial quality control by fusion, fission, and autophagy. Summarizing, aforementioned mechanisms reduced intracellular mutant ataxin-3 protein aggregation to achieve therapeutic effectiveness in the SCA3 model.

Introduction

Spinocerebellar ataxia type 3 (SCA3), also known as Machado-Joseph disease (MJD), is the most common dominantly inherited ataxia for which no effective treatment is currently available. Pathologically, SCA3 may be caused by an expansion of the cytosine–adenine–guanine (CAG) repeat in the *ATXN3* gene. Healthy populations have up to 40 CAG repeats, whereas individuals who develop SCA3 typically have between 55 and 80 repeats[1]. This mutation produces ataxin-3, a large polyglutamine (polyQ) protein that easily aggregates and deposits in neurons in the cerebellum and brainstem, leading to neuronal cell loss [2]. Numerous scholars have identified autophagic dysfunction [3] [4], impaired oxidative stress [5, 6], and mitochondrial bioenergetics [7, 8] as the hallmarks of polyQ disease.

Autophagy is a complex pathway that plays an essential role in maintaining cellular homeostasis in neurodegenerative diseases. Through autophagy, aggregated and misfolded proteins are degraded to maintain cellular homeostasis. However, when autophagy is dysfunctional, damaged or dysfunctional components cannot be properly degraded or cleared, resulting in the accumulation of abnormal protein toxicity. Moreover, the aggregation of ataxin-3 protein exacerbates the problem of dysfunctional autophagy[9]. Beclin1, p62, and Light Chain 3 (LC3), which are key proteins involved in autophagy, have been demonstrated to be dysregulated in SCA3-diseased brains in vivo and in vitro models [10, 11].

Numerous research reports have suggested that oxidative stress plays a key role in the pathogenesis of neurodegenerative diseases [12, 13]. Oxidative stress is a condition caused by an imbalance between the

production and elimination of reactive oxygen species (ROS). Protein misfolding and aggregation can exacerbate ROS production [14], resulting in damage to cellular components. In addition, the generation of ROS is linked to the inactivation of antioxidant systems. Antioxidants can be endogenous (produced by the body) or exogenous (obtained through diet). Endogenous antioxidants, such as glutathione (GSH), superoxide dismutase (SOD), and catalase (CAT), play crucial roles in providing protection against oxidative stress [15]. Antioxidants have been demonstrated to reduce aggregation and cell death in various polyQ disease models[16].

Mitochondrial dysfunction is also considered a pathogenesis of neurodegenerative diseases. Mitochondria are present in all eukaryotic cells and involved in ROS metabolism, adenosine triphosphate (ATP) production, and apoptosis[17]. Although excessive amounts of ROS can harm mitochondrial energy production, mitochondria are a major source of endogenous ROS during cellular respiration and are therefore essential to various cellular functions [18]. When they are present in moderate amounts, mitochondrial ROS trigger the antioxidant compensation mechanism, thereby contributing to metabolic balance[19]. Several studies have indicated that the brain is an organ that consumes considerable amounts of oxygen and energy and that the oxygen consumption of the brain is impaired in patients with neurodegenerative diseases [20, 21]. Furthermore, mitochondrial dynamics play an essential role not only in regulating the morphology and primary functions of organelles but also in their transport (i.e., fusion and fission; [22]. An increase in oxidative stress causes an imbalance of mitochondrial fission and fusion, which is frequently associated with mitochondrial fragmentation, resulting in mitochondrial dysfunction [23].

Astragaloside IV (AST), a major bioactive compound derived from Astragali Radix (*Huangqi* in Chinese) [24], has neuroprotective, anti-inflammatory, and neuroregenerative properties[25–27]. The efficacy of AST has also been described in experimental models of various neurodegenerative diseases [28]. AST triggers the induction of autophagy and therefore has an antiapoptotic effect and protects against cartilage degeneration[29], maintains mitochondrial membrane potential (MMP), increases ATP production [30], and activates Nuclear factor erythroid 2-related factor 2 (Nrf2) signaling to protect neurons [31].

To the best of our knowledge, no study has yet evaluated treatment with AST for SCA3. Using an SCA3 cell model, we determined that AST can be used as a medication for treating SCA3 because of its ability to reduce mutant ataxin-3 protein levels (including aggregation), reduce oxidative stress, and increase mitochondrial function. Our in vivo findings obtained using an SCA3 transgenic mouse model reveal that AST can alleviate motor dysfunction and increase the survival of Purkinje cells.

Materials and Methods

Cell Culture and Treatment

Human neuroblastoma cell lines (SK-N-SH) stably transfected with the full-length ataxin-3 gene with 26 (MJD26) or 78 CAG repeats (MJD78) were provided by Prof. Mingli Hsieh (Department of Life Science, Tunghai University, Taiwan). The cells were grown in Dulbecco's modified Eagle medium (DMEM; high glucose, DMEM-HG, GIBCO/Invitrogen, Carlsbad, CA, USA) containing 10% heat-inactivated fetal bovine serum (HyClone Laboratories, Logan, UT, USA), 1% penicillin/streptomycin (GIBCO, Thermo Fisher Scientific, Inc., Waltham, MA, USA), 1% L-glutamine (GIBCO), 1% non-essential amino acids (GIBCO), and 100-μg/mL G418 (InvivoGen, San Diego, CA, USA) at 37°C in a humidified atmosphere of 5% CO_2. The culture medium was replaced every 2–3 days. The cells were allowed to adhere and grow to 85% confluency for 24 h before experiments were performed. AST (purity: high-performance liquid chromatography value > 98%, U-04410-8-100MG; Sigma-Aldrich, St. Louis, MO, USA) was dissolved in dimethylsulfoxide (DMSO) to the concentration of 80 mg/mL as a stock solution. The maximum final concentration of DMSO in the medium was maintained at 0.1% to ensure the cell viability would not be affected. The cells were exposed to various doses of AST for 24 h.

Protein Aggregation Assay

Aggregation was measured using PROTEOSTAT Protein Aggregation Assay (ENZ-51023-KP002, Enzo Life Sciences, PA, USA) per the manufacturer's instructions. In brief, after being treated for 24 h, the cells were washed with phosphate-buffered saline (PBS), trypsinized with 0.05% trypsin, and collected into PBS. Diluted PROTEOSTAT detection reagent was dispensed into 96-well microplates, after which the protein of interest was added to each well and incubation was performed in the dark for 15 min at room temperature (RT). Fluorescence intensity was measured using a CLARIOstar microplate reader; the reader's excitation wavelength and emission filter were set to approximately 550 and 600 nm, respectively.

Western Blot Analysis

The cells were treated for 24 h, washed with PBS, and trypsinized with 0.05% trypsin, after which their cell lysates were extracted using Pierce IP Lysis Buffer (#87788; Thermo Scientific, MA, USA) supplemented with the protease inhibitor cocktail Set I (#539131; Calbiochem, Billerica, MA) and Phosphatase Inhibitor Cocktail Set V 50x (#524629, Merck Millipore, MA USA). After the cells were lysed on ice for 30 min, they were centrifuged at 14,000 rpm and 4°C for 30 min. The supernatants were collected, and the protein concentration was determined using the Pierce BCA Protein Assay Kit (#23227, Thermo Scientific). The obtained samples were mixed with AllBio 6X SDS Loading Dye (AllBio Science, ABMBD-001, Taiwan) and denatured at 95°C for 5 min. The proteins (20 to 40 μg/lane) were separated using SDS-PAGE gels (10%, #1610183; 12%, #1610185; Bio-Rad, CA, USA), transferred to PVDF membranes (#1704272; Bio-Rad), blocked with blockEBL blocking buffer (MPR-02100, Taipei, Taiwan) for 1 h at RT, and incubated with the following primary antibodies overnight at 4°C: optic atrophy 1 (OPA1, #612607, 1:500; BD Biosciences, San Jose, CA, USA), mitofusin 2 (MFN2, M6319, 1:500; Sigma-Aldrich), p-Drp1 (#3455, 1:250; Cell Signaling, Danvers, MA, USA), dynamin-related protein 1 (Drp1, ab154879, 1:500; Abcam, Cambridge, MA, USA), mitochondrial fission protein 1 (Fis1, ab71498, 1:500; Abcam), translocase of inner mitochondrial membrane 23 (Tim23, #611222, 1:500; BD Biosciences), glyceraldehyde 3-phosphate dehydrogenase

(GAPDH, ab9484, 1:1000; Abcam), ataxin-3 (ab175265, 1:500; Abcam), Beclin1 (NB110-87318, 1:1000; Novus Biologicals, Littleton, CO, USA), p62 (ab56416, 1:1000; Abcam), and LC3 (Cell Signaling, #4108, 1:500). The obtained membranes were washed with tris-buffered saline with Tween 20 and incubated for 1 h with HRP-conjugated secondary antibodies at RT (1:10000; Jackson Immuno Research Laboratories, PA, USA). After the membranes were washed, signals were visualized using the Immobilon Western Chemiluminescence HRP substrate (WBKLS0500, Merck Millipore) and a Fusion-FX7-826.WL Superbright Transilluminator (Vilber Lourmat, Eberhardzell, Germany). The obtained bands were quantified using the imaging processing software ImageJ (Rasband, W.S., National Institutes of Health, Bethesda, MD, USA).

Cell Viability

MJD26 (15000/well) and MJD78 (20000/well) cells were seeded in transparent 96-well plates and incubated overnight. The cells were then treated with various concentrations of AST (12.5, 25, 50, or 100 μM) and incubated for 24 h. After the medium was removed, the cells were incubated in fresh medium with 10% WST-1 reagent (11644807001, Roche, Basel, Switzerland) for 3 h. Absorbance was measured at 450 nm by using a multiplate reader, and a reference wavelength of 690 nm was used; the absorbance value at 690 nm was subtracted from that at 450 nm. The relative cell viability percentage in each group was calculated using comparisons with the cell viability of the control group.

Oxidative Stress and Mitochondrial Membrane Potential

The cells were treated with AST per the procedure as described above. Dihydrofluorescein diacetate (DCF, 1 μM; Invitrogen, Waltham, MA, USA) staining, dihydroethidium (DHE, 10 μM; Invitrogen) staining, MitoSOX Red (5 μM; Invitrogen) staining, and tetramethylrhodamine ethyl ester perchlorate (TMRE, 100 nM; Invitrogen) staining were used to quantify total ROS, mitochondrial superoxide, superoxide ROS, and MMP, respectively. Fluorescence intensity was measured using a FACSCalibur flow cytometer (FC500, Beckman Coulter, Miami, FL, USA).

Antioxidant Enzyme Activity Assay

The cells were treated with AST per the procedure described in a previous subsection. Total GSH, SOD, glutathione peroxidase (GPx), and CAT were measured using a total GSH colorimetric assay kit (E-BC-K097-M; Elabscience Biotechnology, TX, USA), an Amplite colorimetric SOD assay kit (#11305; AAT Bioquest, Sunnyvale, CA, USA), a GPx activity assay kit (E-BC-K096-M; Elabscience Biotechnology), and a CAT activity assay kit (E-BC-K031-M; Elabscience Biotechnology), respectively, per the manufacturers' instructions; detection was performed using a CLARIOstar microplate reader (BMG LABTECH, Offenburg, Germany).

Mitochondrial Respiration

The respiration rates of mitochondria in MJD26 and MJD78 cells were measured at 37°C using a high-resolution Oroboros Oxygraph 2K respirometer (O2k; Oroboros, Innsbruck, Austria) per the procedure described in another study[32]. In brief, 0.5-mM malate and 10-mM L-glutamate were added to obtain the basal respiration rate of the mitochondrial electron transport chain (Routine), 2.5-mM adenosine

diphosphate was added to induce complex I–linked oxidative phosphorylation (OXPHOS), 10-mM succinate was added to enable observation of CI + II-linked OXPHOS (maximum OXPHOS [Max-Ox]), 5-μM oligomycin was added to inhibit ATP synthase, and 1.5-μM FCCP was added to determine the maximum noncoupled respiration (Max-U). Finally, 0.5-μM rotenone and 5-μM antimycin A were added to block respiratory electron flux at mitochondrial complexes I and III to completely shut down mitochondrial oxygen consumption and enable measurement of residual oxygen consumption (ROX).

Animal Model

SCA3 15Q transgenic mice were donated by Prof. Henry L. Paulson (Department of Neurology, University of Michigan, Ann Arbor, MI, USA), and SCA3 84Q transgenic mice were purchased from Jackson Laboratory (Bar Harbor, ME, USA). All transgenic mice used in the present study were of the C57BL/6J strain, and their strain was confirmed through polymerase chain reaction (PCR) analysis conducted using DNA isolated from mouse tail samples obtained at the time of weaning. The primers used for genotyping were identical to those described in another study [33]. The mice were housed in a controlled environment with a 12-h light/dark cycle, and they were provided with ad libitum access to food and water. All animal experiments in the present study were approved by the Institutional Animal Care and Use Committee of Changhua Christian Hospital (approval No. CCH-AE-108-021, July 3, 2020). The mice were randomly assigned to one of three groups (n = 6 per group), namely SCA3 15Q, which comprised mice treated with corn oil (10% DMSO); SCA3 84Q mice, which comprised mice treated with corn oil (10% DMSO); and SCA3 84Q + AST50 mice, which comprised mice treated with AST at a dose of 50 mg/kg/week dissolved in corn oil (10% DMSO). When the mice reached the postnatal age of 6 months, they were orally administered either a vehicle or AST for 12 months. Subsequently, the mice were sacrificed through carbon dioxide asphyxiation, and their cerebellum tissues were promptly extracted and quickly frozen.

Rotarod Test

Motor coordination and balance were measured per the procedure described in another study [34]. In brief, the mice were placed on a rod turning at a constant speed of 5 rpm, and subsequently, the speed of the turning was accelerated linearly from 5 to 40 rpm within 300 s. The latency to fall was quantified as the number of seconds a mouse could remain on the rod. To prevent fatigue, each mouse was allowed to rest for at least 20 min in between trials. A total of six trials were conducted for each mouse, and their latency to fall was recorded and analyzed statistically.

Histopathological Analysis

The hemibrains of the mice were harvested, fixed with 4% paraformaldehyde for 48 h, and dehydrated. For embedding, sectioning, and hematoxylin and eosin (H&E) staining, tissues were processed per the procedure described in another study (10.1007/s12311-018-0936-3). Slides were photographed using a microscope (Olympus, Tokyo, Japan), the entire cerebellar cortex was digitized for each sagittal section, and Purkinje cells were analyzed using ImageJ (Rasband, W.S., National Institutes of Health). The average number of Purkinje cells in the lobules of the Purkinje cell layer in the cerebellum was counted.

Statistical analysis

All experiments were conducted at least in triplicate. In vivo data are presented as means ± standard deviations, whereas in vitro data are presented as means ± standard errors of the mean. Two-tailed Student's *t* tests were performed to identify significant differences between groups (see Figure Legends). A value of $p < 0.05$ was regarded as statistically significant, and such values are indicated in the figures with an asterisk.

Results

Effects of AST on protein aggregation and autophagic clearance of mutant ataxia-3

To explore the potential of AST for treating SCA3, protein aggregation was assessed using a PROTEOSTAT Protein Aggregation Assay kit. The results reveal that the examined MJD78 cells exhibited a higher level of protein aggregation relative to the examined MJD26 cells. AST treatment significantly reduced the percentage of protein aggregation at all examined dose levels (Fig. 1A). To further confirm the ability of AST to eliminate the mutant form of ataxin-3 protein, protein expression was tested through Western blotting. The MJD78 cells expressed the mutant form of ataxia-3 protein, which is caused by the expansion of the CAG repeat encoding of polyQ; however, this phenomenon was not observed in the MJD26 cells. The incubation of MJD78 cells with AST resulted in a dose-dependent reduction in mutant ataxin-3 protein levels, especially when the dosages were high (Fig. 1B). Compared with the MJD26 cells, the MJD78 cells exhibited reduced levels of autophagy-related protein Beclin1 and reduced LC3-II conversion (LC3-II to LC3-I ratio) and increased p62 accumulation. By contrast, a low dose of 12.5 μM AST increased the level of Beclin1 and the LC3-II/I ratio, and a dose of only 50 μM AST significantly increased the autophagy flux, as indicated by the finding of decreased accumulation of p62 (Fig. 1C). This finding demonstrates that the increased autophagy induced by 50 μM of AST was related to this dose of AST leading to more effective removal of mutant protein accumulation.

Effects of AST on cell viability and oxidative stress

To test whether AST exhibits cytotoxicity, the cells were treated with various doses of AST (0, 12.5, 25, or 50 μM) for 24 h. Figure 1A reveals the absence of any significant difference in cell viability between the MJD26 and MJD78 cells after 24 h of treatment; this result, which was verified using a WST-1 assay, highlights the safety of AST. Furthermore, we discovered that the MJD78 cells exhibited a significant upregulation of oxidative stress relative to the MJD26 cells. After the MJD 78 cells underwent AST treatment, their total ROS, superoxide ROS, and mitochondrial ROS decreased, particularly when 50 μM AST was used.

Effects of AST on antioxidant capacity

To enable assessment of antioxidant capacity, the MJD78 cells treated with various doses of AST were comprehensively evaluated for enzymatic antioxidants, including GSH (Fig. 2A), SOD (Fig. 2B), GPx

(Fig. 2C), and CAT (Fig. 2D). The data presented in Fig. 3 reveal a considerable decrease in antioxidant system activity in the MJD78 cells. The levels of all antioxidant-related molecules increased consistently and significantly at all tested doses of AST in a non-dose-dependent manner.

Effects of AST on mitochondrial respiration and dynamic-related proteins

To explore the potential effects of AST on the mitochondrial function of MJD78 cells, we measured the MMP, mitochondrial respiration, and levels of mitochondrial-shaping protein. First, the relative fluorescence of TMRE was used to determine the MMP, and the results reveal a significantly higher TMRE fluorescence in the MJD26 cells than in the MJD78 cells. However, after the cells underwent AST treatment for 24 h, the MMP was revealed to be upregulated in the MJD78 cells, with notable increases observed at AST doses of 12.5 and 50 μM (Fig. 3A). Second, we used O2k to measure oxygen consumption (O_2 flux) and assess the overall mitochondrial respiration in the MJD26 and MJD78 cells. Several quantification parameters of O_2 flux, including basal respiration (Routine), OXPHOS, and Max-Ox, were significantly lower in the MJD78 cells than in the MJD26 cells; however, this phenomenon was not identified for Max-U. After AST treatment was administered, the Routine, OXPHOS, and Max-Ox of O_2 flux significantly increased (Fig. 3B). Third, we assessed mitochondrial proteins through Western blotting. Mitochondrial dynamics (fusion and fission) maintain the integrity of the mitochondrial network. MFN2 and OPA1 are mitochondrial fusion proteins, whereas Fis1 and Drp1 are mitochondrial fission proteins. The levels of phosphor-Drp1 and Fis1 proteins were significantly higher in the MJD78 cells than in the MJD26 cells, whereas the expression of MFN2, OPA1, and Tim23 proteins remained unchanged. After AST treatment was administered, the expression of both mitochondrial fusion and mitochondrial fission proteins was downregulated, indicating that mitochondrial homeostasis had been stabilized (Fig. 3D).

Effects of AST on rotarod performance and cerebellar Purkinje cell numbers in SCA3 mice

To further validate the protective effects of AST, the motor function of the SCA3 transgenic mice used in the present study was evaluated by assessing their rotarod performance and the number of Purkinje cells in their cerebellums. The mice started undergoing rotarod testing at the age of 6 months and were subsequently tested every month for 12 months while undergoing AST intervention. Notably, at the age of 6 months, the latency to fall was significantly shorter among the SCA3 84Q mice than among the SCA3 15Q mice. However, after 12 months of AST treatment, the AST-treated SCA3 84Q mice consistently improved in terms of their average latency to fall (Fig. 5A). After normalization to the pretreatment point was performed, the relative latency to fall remained higher in the AST-treated SCA3 84Q mice than in the nontreated SCA3 84Q mice (Fig. 5B). After the mice were sacrificed, their cerebellar sections were used for histopathological analysis to visualize the individual Purkinje cell layer. Through H&E staining, the appearance and number of the examined Purkinje cells were revealed to be significantly damaged and reduced, respectively (Fig. 5C). That is, the average number of Purkinje cells per 100 μM was quantified,

and the results revealed a significantly lower cell number in the SCA3 84Q mice than in the SCA3 15Q mice. The administration of AST, however, reverted this declining trend, clearly demonstrating the protective effect of AST (Fig. 5D).

Discussion

The therapeutic effects of AST on SCA3 were validated using multiple models. The results consistently indicated that AST treatment provided several benefits, namely reducing protein aggregation and mutant ataxin-3 protein expression, ameliorating mitochondrial function and increasing the antioxidant capacity of MJD78 cells (Fig. 6), and increasing the locomobility and survival of cerebellar Purkinje cells in SCA3 84Q mice. These mechanisms could be related to the activation of the autophagy-mediated clearance of mutant proteins (defined in our previous study) in the MJD78 cell line during Nrf2 agonist treatment[32].

The expansion of polyQ can increase the aggregation propensity of mutant proteins, and the progressive formation of insoluble protein aggregates is a hallmark of numerous neurodegenerative diseases [35]. The available body of evidence strongly indicates the presence of abnormalities in the functionality of autophagy, which causes the degradation of misfolded proteins [36]. Studies have reported impaired autophagy in the brains of patients with SCA3 and significantly decreased levels of Beclin1 during the initial formation of autophagosomes[10]. In addition, research indicates other autophagy biomarkers (e.g., p62 and LC3. p62) are activated upon stress induction, enabling selective autophagic flux, and LC3 protein plays a crucial role in autophagy in that it facilitates autophagosome elongation and closure[37]. The accumulation of p62 protein is typically regarded as an indicator of autophagy inhibition [38], and the clearance of mutant ataxin-3 protein through autophagy may be hindered by various factors. In the present study, the protein expression of Beclin1 and the LC3-II/I ratio were lower and the level of p62 was higher in the MJD78 cells than in the MJD26 cells. After AST treatment was administered, the trends for protein aggregation, mutant ataxin-3 protein expression, and autophagic flux were reversed, suggesting that the beneficial effects of AST could be related to the induction of autophagy in the MJD78 cells. Although the present study did not yield conclusive evidence regarding the effect of AST in reducing mutant protein accumulation through AST-activated autophagy, Liu et al. reported that AST-mediated autophagy plays an antiapoptotic role, protecting cells from interleukin-1β-induced cartilage degeneration [29]. Further research is required to approve the protective mechanism of AST in enhancing autophagy against neurodegenerative diseases.

ROS include free radicals such as O_2^-, non-radicals such as H_2O_2, and the hydroxyl radical. ROS production at an appropriate level plays a physiological role in cellular differentiation and proliferation, whereas ROS expression at a level that exceeds physiological limits results in oxidative stress [39]. The overproduction of ROS and impaired antioxidant activity are accelerated by neurodegenerative diseases, which leads to disease progression. Of the types of ROS, O_2^- is considered one of the greatest contributors to ROS production [40]. Our results indicate that both intracellular and superoxide ROS were significantly increased in the MJD78 cells relative to the MJD26 cells. This increase was significantly reversed by AST treatment administered at the concentration of 50 μM. This finding highlights the role of

AST in mitigating the oxidative stress associated with neurodegeneration. The neuroprotective effects of AST are associated with reduced oxidative stress. Gui et al. demonstrated that AST reduced the high glucose–induced ROS production and oxidative stress in podocytes[41]. In the present study, a high dose of AST (100 μM) increased the levels of cellular ROS (Supplementary Fig. 1). This finding is consistent with that reported by Sun et al., who employed a neural cell model of Alzheimer's disease and reported that Treatment concentration of AST at less than 50 μM improved cell survival and reduced Amyloid-β-induced neurotoxicity but had the opposite effect when the concentration was increased to 100 μM [42]. Therefore, when AST is used to treat neurodegenerative diseases, the proper dosage for minimizing potential counter-effects must be considered. Protection against oxidative stress is dependent on endogenous antioxidants, including GSH, SOD, GPx, and CAT. However, neurons have been demonstrated to exhibit a weaker antioxidant defense and limited regenerative capacity relative to other tissue cells[43]. In the present study, the expression of the aforementioned endogenous antioxidants was revealed to be lower in the MJD78 cells than in the MJD26 cells, indicating dysfunction in the antioxidant system. After AST treatment was administered, the levels of antioxidant-related molecules increased, demonstrating that AST can restore antioxidant capacity and potentially counteract the detrimental effects of oxidative stress in individuals with neurodegenerative conditions.

Substantial evidence indicates that both oxidative stress and mitochondria are key factors in the pathogenesis of neurodegenerative disorders [44]. Oxidative stress can directly affect mitochondrial function, which primarily involves generating ATP for energy and is closely related to bioenergetics and oxidative phosphorylation. The brain comprises billions of neurons that create complex networks through electrical and chemical signals, and this process is energy intensive [45]. Thus, in numerous neurodegenerative disorders, mitochondrial dysfunction has been implicated in SCA3 disease progression [46]. Dysfunctional mitochondria disrupt the key energy production processes within neurons, leading to impaired neuronal function. The key indicators for maintaining mitochondrial quality include the MMP, oxygen consumption rate, and mitochondrial dynamics. The MMP plays a crucial role in the functioning of mitochondria, and it drives ATP synthesis by facilitating the flow of protons [47]. Compared with the fibroblasts from healthy individuals, those from individuals with SCA3 contain fragmented and circular mitochondria in addition to lower levels of OXPHOS complexes, ATP production, and cell viability [7]. This phenomenon is consistent with our results, which indicate that the MMP and level of mitochondrial respiration, including Routine, OXPHOS, and Max-Ox, were significantly lower in the MJD78 cells we examined than in the MJD26 cells we examined. Notably, after AST treatment was administered, the MMP and mitochondrial respiration were restored in the cells. In addition, although the effects of AST on mitochondrial dynamics remain unclear, in the present study, the levels of mitochondrial fission proteins, p-Drp1, and Fis1 were significantly higher in the examined MJD78 cells than in the examined MJD26 cells but lower after AST treatment, and this treatment process did not affect the amount of mitochondria, as indicated by the results regarding the expression of the inner membrane protein Tim23 and mitochondrial DNA copy number (Supplementary Fig. 2). Abnormal mitochondrial dynamics characterized by excessive numbers of mitochondrial fragments has been reported in various models of SCA3 [48, 49]. The processes of mitochondrial fission and fusion have been

widely reported to play an essential role in preserving the functionality of mitochondria [50]. A study reported that decreased mitochondrial fragmentation and increased mitochondrial elongation were observed in neural neuroblastoma cells of SCA3 that were treated with far-infrared radiation [48]. The present results reveal that the regulatory effect of AST is related to the regulation of mitochondrial function, including respiratory efficiency and dynamic performance.

To further validate the efficacy of AST in vivo, preliminary tests were conducted, with SCA3 84Q transgenic mice used as a model for potential treatments. These transgenic mice underwent notable physical changes characterized by balance instabilities similar to the clinical manifestations of SCA3 in humans. In the present study, the doses of AST that were administered were based on those used by Yin et al., who investigated treatment for cerebral ischemia. Yin et al. reported that administering AST for 7 days at dose of 50 mg/kg/day effectively prevented neuronal apoptosis in rats with ischemia-reperfusion injury [51]. The neuroprotective effects of AST have also been demonstrated in disease models. Lin et al. demonstrated the effectiveness of AST in improving spinal cord recovery and enhancing locomotor function in rats with spinal cord injury [52]. Chen et al. reported that AST ameliorated cognitive impairment, neuroinflammation, and neuronal damage in a mouse model of oligomeric Amyloid-β-induced Alzheimer's disease [27]. Xia et al. demonstrated that AST significantly alleviated behavioral deficiencies in a mouse model of Parkinson's disease induced by 1-methyl-4-phenyl-1,2,3,6-tetrahydropyridine [53]. In our study, we revealed that AST improved motor dysfunction in SCA3 transgenic mice and prevented the loss of Purkinje neurons in their cerebellums. Although these results provide insights that can aid in the development of therapeutic strategies for patients with SCA3, additional studies are required to further clarify the protective role of AST in regulating SCA3 disease progression.

In summary, the present study provides in vitro and in vivo evidence of the effects of AST treatment on SCA3. The in vitro mechanism of action of AST is associated not only with decreased protein aggregation and mutant ataxin-3 protein expression but also with decreased oxidative stress and enhanced mitochondrial function. Moreover, our in vivo study verified that AST treatment prevents motor dysfunction and cellular Purkinje cell death. Thus, on the basis of our findings, we suggest the use of AST as a potential therapeutic intervention for impeding SCA3 progression.

Abbreviations

AST	astragaloside IV
ATP	adenosine triphosphate
CAG	cytosine–adenine–guanine
CAT	catalase
DCF	Dihydrofluorescein diacetate
DHE	dihydroethidium
Drp1	dynamin-related protein 1
Fis1	fission protein 1
GAPDH	glyceraldehyde 3-phosphate dehydrogenase
GPx	glutathione peroxidase
GSH	glutathione
H&E	hematoxylin and eosin
LC3	Light Chain 3
Max-U	maximum noncoupled respiration
MFN2	mitofusin 2
MJD	Machado-Joseph disease
MMP	mitochondrial membrane potential
Nrf2	Nuclear factor erythroid 2-related factor 2
OPA1	optic atrophy 1
OXPHOS	oxidative phosphorylation
PBS	phosphate-buffered saline
PCR	Polymerase chain reaction
polyQ	polyglutamine
ROS	reactive oxygen species
ROX	residual oxygen consumption
RT	room temperature
SCA3	spinocerebellar ataxia type 3
SK-N-SH	Human neuroblastoma cell lines
SOD	superoxide dismutase

Tim23	inner mitochondrial membrane 23
TMRE	tetramethylrhodamine ethyl ester perchlorate

Declarations

Acknowledgements

We would like to thank Prof. Mingli Hsieh (Department of Life Science, Tunghai University, Taiwan) for kindly provide the Human neuroblastoma cell lines (SK-N-SH MJD26 and MJD78) and Prof. Henry L. Paulson (Department of Neurology, University of Michigan, Ann Arbor, MI, USA) for kindly provide the hemizygous SCA3 15Q transgenic mice. This manuscript was edited by Wallace Academic Editing.

Author contribution

Yongshiou Lin: performed experiments, analyzed data, and co-wrote the manuscript.

Wenling Cheng: designed experiments, performed experiments, and edited the manuscript.

Juichih Chang: interpreted data and edited the manuscript

Yuling Wu: performed experiments, analyzed data

Mingli Hsieh: provide the Human neuroblastoma cell lines and edited the manuscript.

Chinsan Liu: designed experiments, interpreted data and co-wrote the manuscript.

All authors reviewed the final manuscript.

Funding

This study was sponsored by grants from Ministry of Science and Technology in Taiwan (MOST 109-2314-B-371 -008 -MY3). This research was also supported by Changhua Christian Hospital (110-CCH-MST-168, 110-CCH-MST-123, 111-CCH-MST-117).

Data availability

The data presented in this study are available on request from the corresponding author.

Ethics Approval

All animal studies were conducted in accordance with the National Institutes of Health Guide and European Community directives for the Care and Use of Laboratory Animals and approved by the Institutional Animal Care and Use Committee of Changhua Christian Hospital (CCH-AE-106-017).

Consent of Publication

All authors read and approved the final manuscript.

Conflict of Interest

The authors declare no competing interests.

References

1. Li X, Liu H, Fischhaber PL, Tang T-S (2015) Toward therapeutic targets for SCA3: Insight into the role of Machado–Joseph disease protein ataxin-3 in misfolded proteins clearance. Progress in Neurobiology 132:34-58
2. Ikeda H, Yamaguchi M, Sugai S, Aze Y, Narumiya S, Kakizuka A (1996) Expanded polyglutamine in the Machado–Joseph disease protein induces cell death in vitro and in vivo. Nature genetics 13 (2):196-202
3. Lee J-H, Lin S-Y, Liu J-W, Lin S-Z, Harn H-J, Chiou T-W (2021) n-Butylidenephthalide modulates autophagy to ameliorate neuropathological progress of spinocerebellar ataxia type 3 through mTOR pathway. International Journal of Molecular Sciences 22 (12):6339
4. Paulino R, Nóbrega C (2023) Autophagy in Spinocerebellar Ataxia Type 3: From Pathogenesis to Therapeutics. International Journal of Molecular Sciences 24 (8):7405
5. de Assis AM, Saute JAM, Longoni A, Haas CB, Torrez VR, Brochier AW, Souza GN, Furtado GV, Gheno TC, Russo A (2017) Peripheral oxidative stress biomarkers in spinocerebellar ataxia type 3/Machado–Joseph disease. Frontiers in Neurology 8:485
6. Wu Y-L, Chang J-C, Lin W-Y, Li C-C, Hsieh M, Chen H-W, Wang T-S, Liu C-S, Liu K-L (2017) Treatment with caffeic acid and resveratrol alleviates oxidative stress induced neurotoxicity in cell and drosophila models of spinocerebellar ataxia type3. Scientific reports 7 (1):11641
7. Harmuth T, Weber JJ, Zimmer AJ, Sowa AS, Schmidt J, Fitzgerald JC, Schöls L, Riess O, Hübener-Schmid J (2022) Mitochondrial dysfunction in spinocerebellar ataxia type 3 is linked to VDAC1 deubiquitination. International Journal of Molecular Sciences 23 (11):5933
8. Nan Y, Lin J, Cui Y, Yao J, Yang Y, Li Q (2021) Protective role of vitamin B6 against mitochondria damage in Drosophila models of SCA3. Neurochemistry International 144:104979
9. Vasconcelos-Ferreira A, Carmo-Silva S, Codêsso JM, Silva P, Martinez ARM, França Jr MC, Nóbrega C, Pereira de Almeida L (2022) The autophagy-enhancing drug carbamazepine improves neuropathology and motor impairment in mouse models of Machado–Joseph disease. Neuropathology and Applied Neurobiology 48 (1):e12763
10. Sittler A, Muriel MP, Marinello M, Brice A, den Dunnen W, Alves S (2018) Deregulation of autophagy in postmortem brains of Machado-Joseph disease patients. Neuropathology 38 (2):113-124
11. McLoughlin HS, Moore LR, Paulson HL (2020) Pathogenesis of SCA3 and implications for other polyglutamine diseases. Neurobiology of disease 134:104635

12. Gandhi S, Abramov AY (2012) Mechanism of oxidative stress in neurodegeneration. Oxidative medicine and cellular longevity 2012
13. Singh A, Kukreti R, Saso L, Kukreti S (2019) Oxidative stress: a key modulator in neurodegenerative diseases. Molecules 24 (8):1583
14. Pardillo-Díaz R, Pérez-García P, Castro C, Nunez-Abades P, Carrascal L (2022) Oxidative stress as a potential mechanism underlying membrane hyperexcitability in neurodegenerative diseases. Antioxidants 11 (8):1511
15. Aguilar TAF, Navarro BCH, Pérez JAM (2016) Endogenous antioxidants: a review of their role in oxidative stress. A master regulator of oxidative stress-the transcription factor nrf2:3-20
16. Chen C-M, Chen W-L, Hung C-T, Lin T-H, Lee M-C, Chen I-C, Lin C-H, Chao C-Y, Wu Y-R, Chang K-H (2019) Shaoyao Gancao Tang (SG-Tang), a formulated Chinese medicine, reduces aggregation and exerts neuroprotection in spinocerebellar ataxia type 17 (SCA17) cell and mouse models. Aging (Albany NY) 11 (3):986
17. Mattson MP, Gleichmann M, Cheng A (2008) Mitochondria in neuroplasticity and neurological disorders. Neuron 60 (5):748-766
18. Ulasov AV, Rosenkranz AA, Georgiev GP, Sobolev AS (2022) Nrf2/Keap1/ARE signaling: Towards specific regulation. Life Sciences 291:120111
19. Wang DK, Zheng HL, Zhou WS, Duan ZW, Jiang SD, Li B, Zheng XF, Jiang LS (2022) Mitochondrial dysfunction in oxidative stress-mediated intervertebral disc degeneration. Orthopaedic surgery 14 (8):1569-1582
20. Grimm A, Eckert A (2017) Brain aging and neurodegeneration: from a mitochondrial point of view. Journal of neurochemistry 143 (4):418-431
21. Monzio Compagnoni G, Di Fonzo A, Corti S, Comi GP, Bresolin N, Masliah E (2020) The role of mitochondria in neurodegenerative diseases: the lesson from Alzheimer's disease and Parkinson's disease. Molecular neurobiology 57:2959-2980
22. Belenguer P, Duarte JM, Schuck PF, Ferreira GC (2019) Mitochondria and the brain: bioenergetics and beyond. Neurotoxicity research 36:219-238
23. Pickles S, Vigié P, Youle RJ (2018) Mitophagy and quality control mechanisms in mitochondrial maintenance. Current Biology 28 (4):R170-R185
24. Tang W, Eisenbrand G, Tang W, Eisenbrand G (1992) Astragalus membranaceus (Fisch.) Bge. Chinese Drugs of Plant Origin: Chemistry, Pharmacology, and Use in Traditional and Modern Medicine:191-197
25. Zhang Z-g, Wu L, Wang J-l, Yang J-d, Zhang J, Zhang J, Li L-h, Xia Y, Yao L-b, Qin H-z (2012) Astragaloside IV prevents MPP+-induced SH-SY5Y cell death via the inhibition of Bax-mediated pathways and ROS production. Molecular and cellular biochemistry 364:209-216
26. Zhang X, Chen J (2013) The mechanism of astragaloside IV promoting sciatic nerve regeneration. Neural Regeneration Research 8 (24):2256

27. Chen F, Yang D, Cheng X-Y, Yang H, Yang X-H, Liu H-T, Wang R, Zheng P, Yao Y, Li J (2021) Astragaloside IV ameliorates cognitive impairment and neuroinflammation in an oligomeric aβ induced Alzheimer's disease mouse model via inhibition of microglial activation and NADPH oxidase expression. Biological and Pharmaceutical Bulletin 44 (11):1688-1696
28. Costa IM, Lima FO, Fernandes LC, Norrara B, Neta FI, Alves RD, Cavalcanti JR, Lucena EE, Cavalcante JS, Rego A (2019) Astragaloside IV supplementation promotes a neuroprotective effect in experimental models of neurological disorders: a systematic review. Current neuropharmacology 17 (7):648-665
29. Liu J, Meng Q, Jing H, Zhou S (2017) Astragaloside IV protects against apoptosis in human degenerative chondrocytes through autophagy activation. Molecular medicine reports 16 (3):3269-3275
30. Tan Y-Q, Chen H-W, Li J (2020) Astragaloside IV: an effective drug for the treatment of cardiovascular diseases. Drug Design, Development and Therapy:3731-3746
31. Gu D-m, Lu P-H, Zhang K, Wang X, Sun M, Chen G-Q, Wang Q (2015) EGFR mediates astragaloside IV-induced Nrf2 activation to protect cortical neurons against in vitro ischemia/reperfusion damages. Biochemical and Biophysical Research Communications 457 (3):391-397
32. Wu Y-L, Chang J-C, Chao Y-C, Chan H, Hsieh M, Liu C-S (2022) In Vitro Efficacy and Molecular Mechanism of Curcumin Analog in Pathological Regulation of Spinocerebellar Ataxia Type 3. Antioxidants 11 (7):1389
33. Lin Y-T, Lin Y-S, Cheng W-L, Chang J-C, Chao Y-C, Liu C-S, Wei A-C (2021) Transcriptomic and metabolic network analysis of metabolic reprogramming and IGF-1 modulation in SCA3 transgenic mice. International Journal of Molecular Sciences 22 (15):7974
34. Lin Y-S, Cheng W-L, Chang J-C, Lin T-T, Chao Y-C, Liu C-S (2022) IGF-1 as a potential therapy for spinocerebellar ataxia type 3. Biomedicines 10 (2):505
35. Orr HT (2012) Polyglutamine neurodegeneration: expanded glutamines enhance native functions. Current opinion in genetics & development 22 (3):251-255
36. Nascimento-Ferreira I, Santos-Ferreira T, Sousa-Ferreira L, Auregan G, Onofre I, Alves S, Dufour N, Colomer Gould VF, Koeppen A, Déglon N (2011) Overexpression of the autophagic beclin-1 protein clears mutant ataxin-3 and alleviates Machado–Joseph disease. Brain 134 (5):1400-1415
37. Ma S, Attarwala IY, Xie X-Q (2019) SQSTM1/p62: a potential target for neurodegenerative disease. ACS chemical neuroscience 10 (5):2094-2114
38. Bortnik S, Gorski SM (2017) Clinical applications of autophagy proteins in cancer: from potential targets to biomarkers. International journal of molecular sciences 18 (7):1496
39. Checa J, Aran JM (2020) Reactive oxygen species: drivers of physiological and pathological processes. Journal of Inflammation research:1057-1073
40. Kim GH, Kim JE, Rhie SJ, Yoon S (2015) The role of oxidative stress in neurodegenerative diseases. Experimental neurobiology 24 (4):325

41. Gui D, Guo Y, Wang F, Liu W, Chen J, Chen Y, Huang J, Wang N (2012) Astragaloside IV, a novel antioxidant, prevents glucose-induced podocyte apoptosis in vitro and in vivo. PloS one 7 (6):e39824
42. Sun Q, Jia N, Wang W, Jin H, Xu J, Hu H (2014) Protective effects of astragaloside IV against amyloid beta1-42 neurotoxicity by inhibiting the mitochondrial permeability transition pore opening. PloS one 9 (6):e98866
43. Sienes Bailo P, Llorente Martín E, Calmarza P, Montolio Breva S, Bravo Gómez A, Pozo Giráldez A, Sánchez-Pascuala Callau JJ, Vaquer Santamaría JM, Dayaldasani Khialani A, Cerdá Micó C (2022) The role of oxidative stress in neurodegenerative diseases and potential antioxidant therapies. Advances in Laboratory Medicine/Avances en Medicina de Laboratorio 3 (4):342-350
44. Yu YC, Kuo CL, Cheng WL, Liu CS, Hsieh M (2009) Decreased antioxidant enzyme activity and increased mitochondrial DNA damage in cellular models of Machado-Joseph disease. Journal of neuroscience research 87 (8):1884-1891
45. Liu Z, Zhou T, Ziegler AC, Dimitrion P, Zuo L (2017) Oxidative stress in neurodegenerative diseases: from molecular mechanisms to clinical applications. Oxidative medicine and cellular longevity 2017
46. Federico A, Cardaioli E, Da Pozzo P, Formichi P, Gallus GN, Radi E (2012) Mitochondria, oxidative stress and neurodegeneration. Journal of the neurological sciences 322 (1-2):254-262
47. Angelova PR, Abramov AY (2018) Role of mitochondrial ROS in the brain: from physiology to neurodegeneration. FEBS letters 592 (5):692-702
48. Chang J-C, Wu S-L, Hoel F, Cheng Y-S, Liu K-H, Hsieh M, Hoel A, Tronstad KJ, Yan K-C, Hsieh C-L (2016) Far-infrared radiation protects viability in a cell model of Spinocerebellar Ataxia by preventing polyQ protein accumulation and improving mitochondrial function. Scientific reports 6 (1):30436
49. Hsu J-Y, Jhang Y-L, Cheng P-H, Chang Y-F, Mao S-H, Yang H-I, Lin C-W, Chen C-M, Yang S-H (2017) The truncated C-terminal fragment of mutant ATXN3 disrupts mitochondria dynamics in spinocerebellar ataxia type 3 models. Frontiers in molecular neuroscience 10:196
50. Youle RJ, Van Der Bliek AM (2012) Mitochondrial fission, fusion, and stress. Science 337 (6098):1062-1065
51. Yin F, Zhou H, Fang Y, Li C, He Y, Yu L, Wan H, Yang J (2020) Astragaloside IV alleviates ischemia reperfusion-induced apoptosis by inhibiting the activation of key factors in death receptor pathway and mitochondrial pathway. Journal of ethnopharmacology 248:112319
52. Lin J, Pan X, Huang C, Gu M, Chen X, Zheng X, Shao Z, Hu S, Wang B, Lin H (2020) Dual regulation of microglia and neurons by Astragaloside IV-mediated mTORC1 suppression promotes functional recovery after acute spinal cord injury. Journal of cellular and molecular medicine 24 (1):671-685
53. Xia L, Guo D, Chen B (2017) Neuroprotective effects of astragaloside IV on Parkinson disease models of mice and primary astrocytes. Experimental and therapeutic medicine 14 (6):5569-5575

Figures

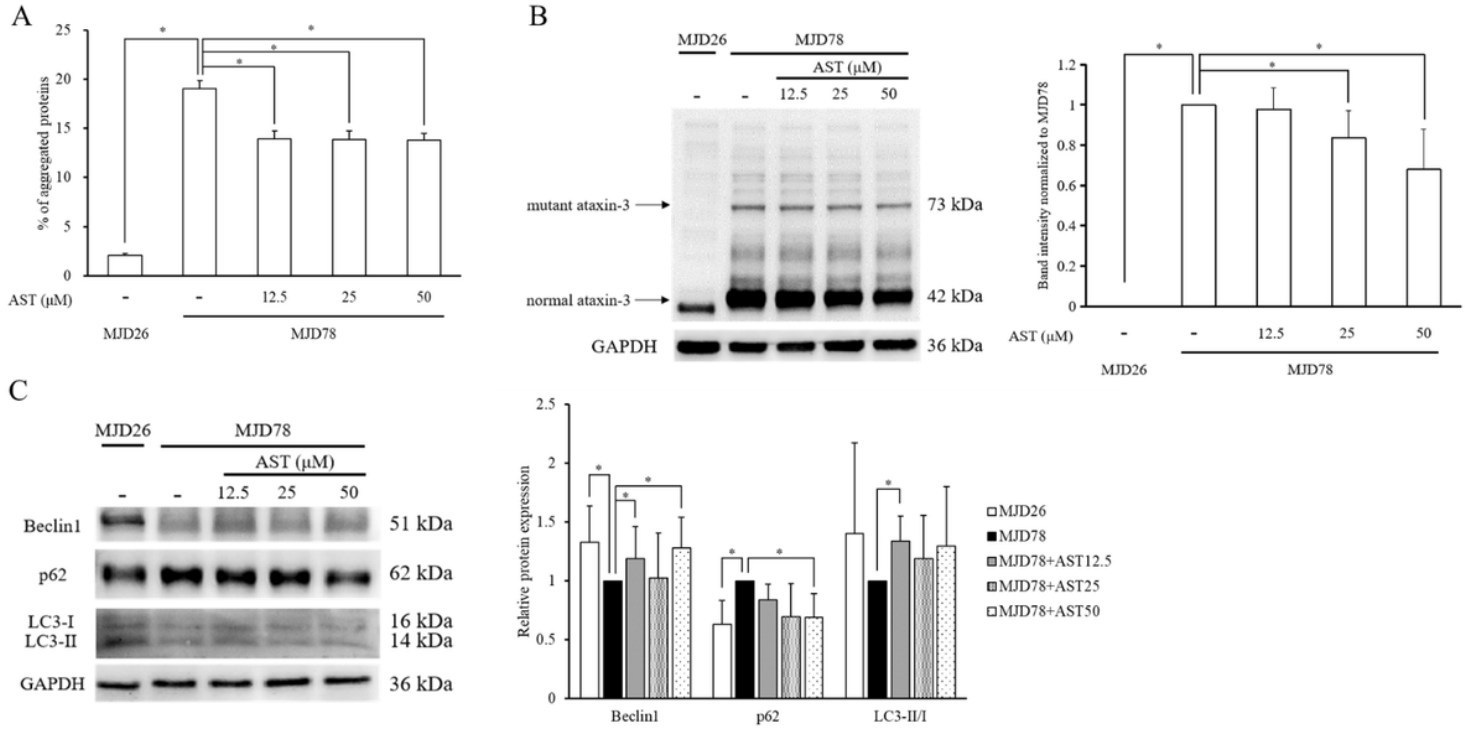

Figure 1

Expression of protein aggregation, ataxin-3 protein, and autophagy-related proteins. Cells were treated with different concentrations of ASTfor 24 h. (A) Assessment of protein aggregation was performed using a PROTEOSTAT Protein Aggregation Assay. (B) The expression of mutant and normal ataxin-3 proteins was investigated through Western blotting. (C) The expression of autophagy markers (Beclin1, p62, and LC3-II/I) was determined through Western blotting. Quantification data were normalized to the expression levels of GAPDH and AST-untreated MJD78 cells. Data are presented as the means ± SDs of more than three independent experiments. * $p < 0.05$.

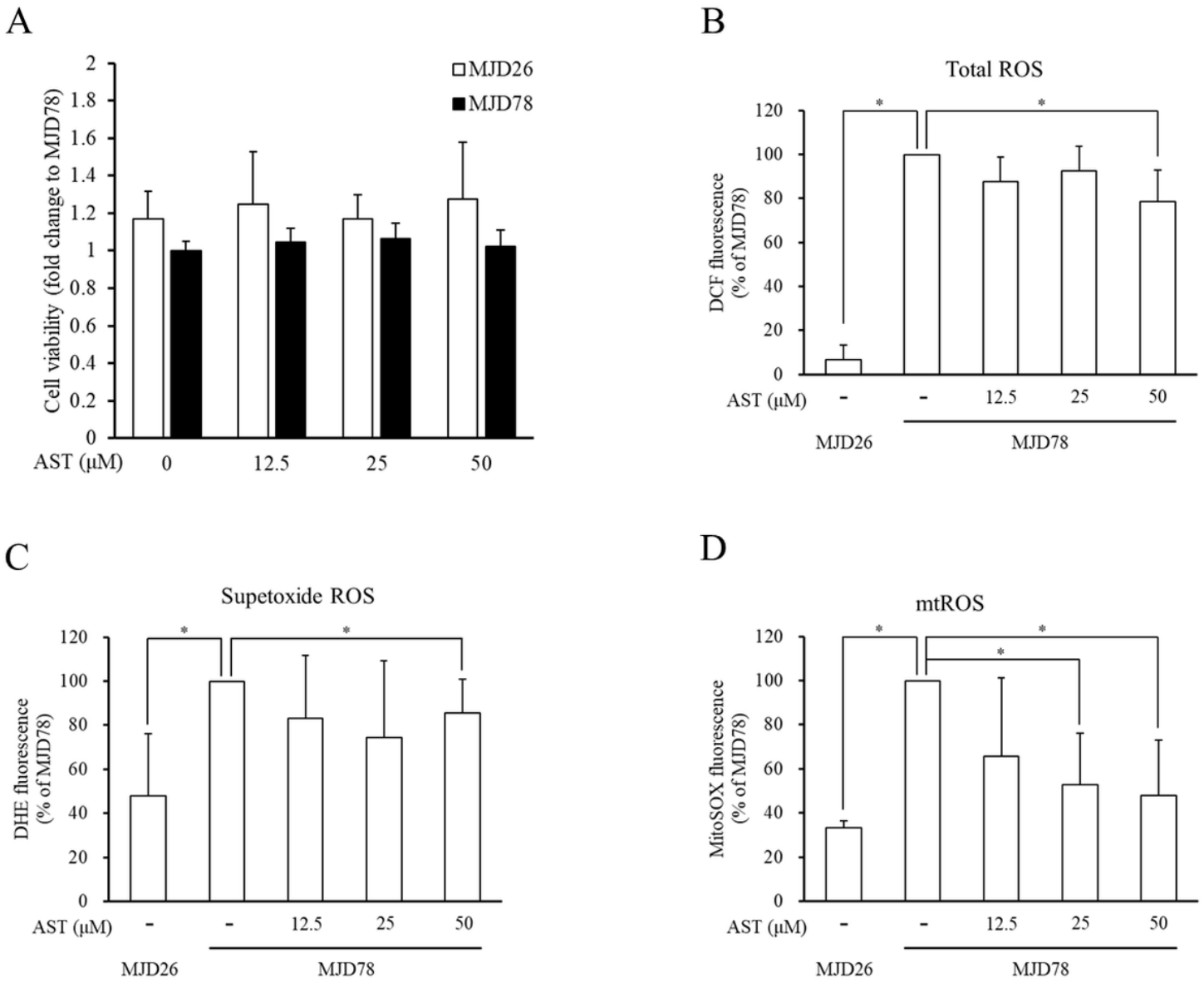

Figure 2

Expression of cell viability and oxidative stress in MJD cells. Cells were treated with different concentrations of AST for 24 h. (A) Cell viability was assessed using WST-1. Oxidative stress was detected through flow cytometry analysis involving (B) DCF staining for intracellular (total) ROS, (C) DHE staining for superoxide ROS, and (D) MitoSOX Red staining for mitochondrial superoxide (mtROS). Data are presented as the means ± SDs of at least three independent experiments. * $p < 0.05$.

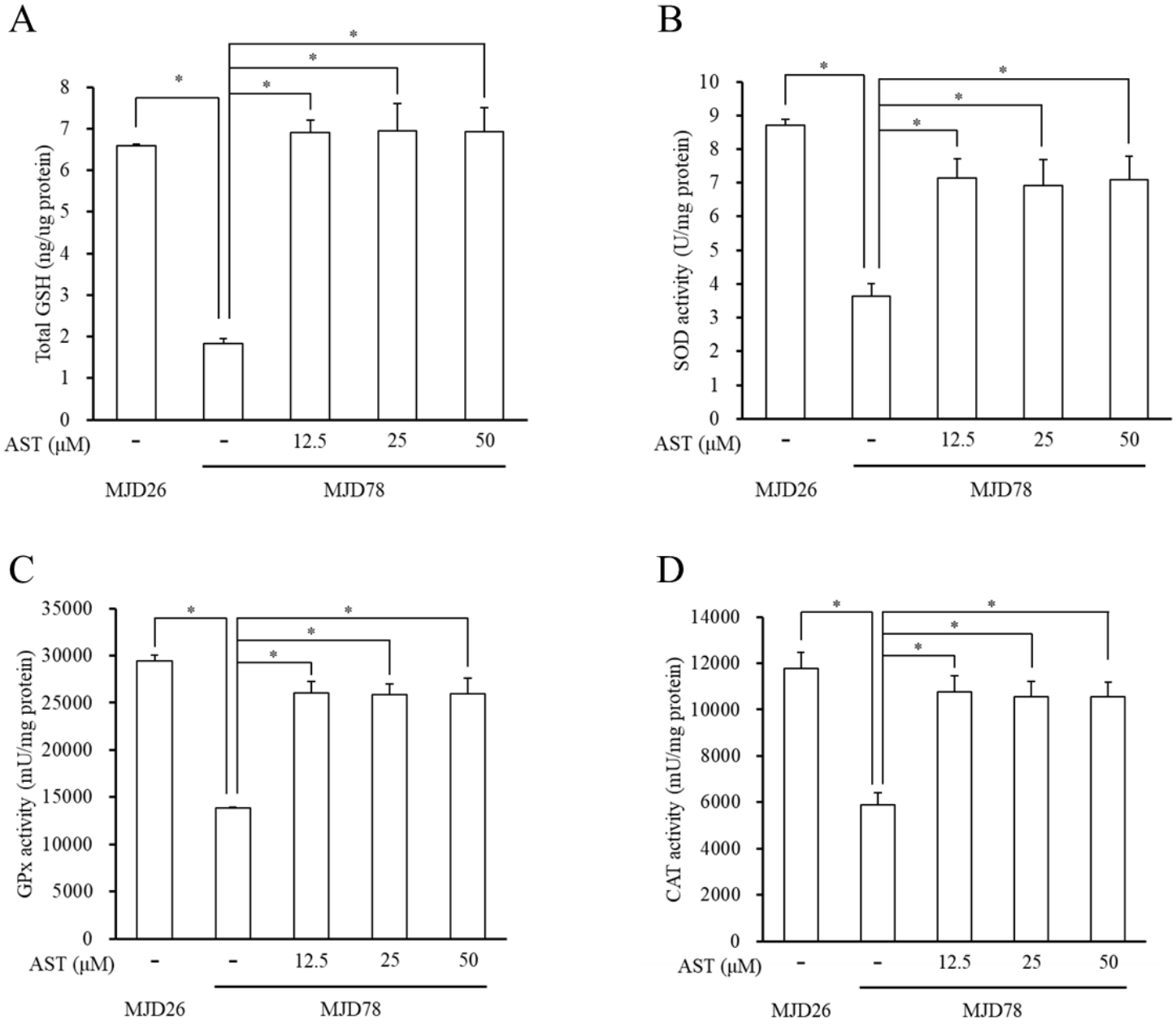

Figure 3

Performance of enzymatic antioxidants in MJD cells. Cells were treated with or without different concentrations of AST for 24 h. Total GSH (A), SOD (B), GPx (C), and CAT (D) were measured with a total GSH colorimetric assay kit, an AmpliteTM colorimetric SOD assay kit, a GSH-Px activity assay kit, and a CAT activity assay kit, respectively, and quantification was performed using a CLARIOstar microplate reader. Data are presented as means ± SDs of three independent experiments. * $p < 0.05$.

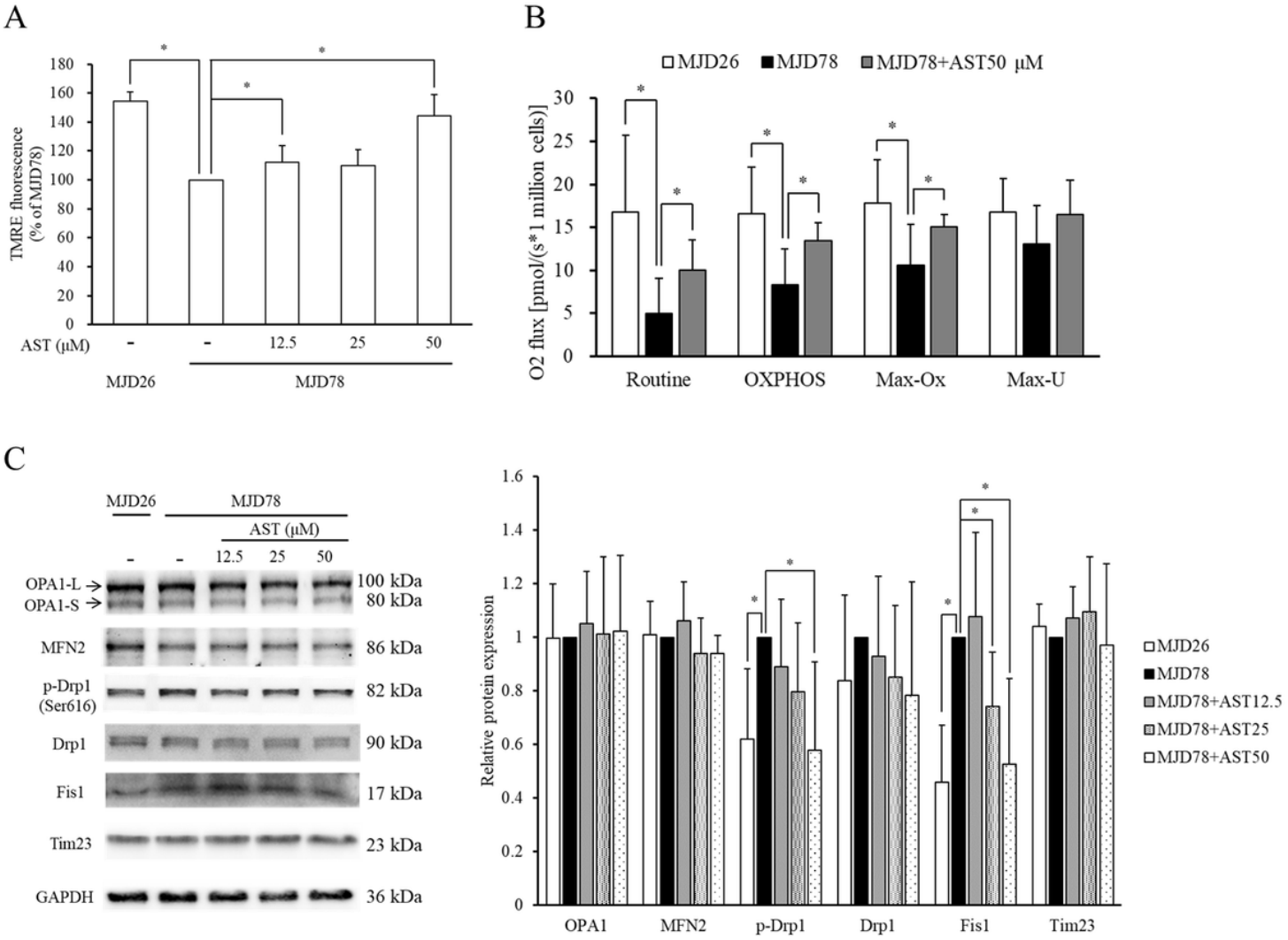

Figure 4

Expression of mitochondrial membrane potential, respiration, and dynamic-related proteins in MJD cells. Cells were treated with or without different concentrations of AST for 24 h. (A) Quantification analysis of MMP was performed through TMRE staining. (B) The rates for Routine, OXPHOS, Max-Ox, and Max-U were determined using O2k. (C) The expression of mitochondrial fusion (OPA1 and MFN2) and fission proteins (Drp1 and Fis1) and a mitochondrial marker protein (Tim23) were detected through Western blotting. Target protein expression levels were normalized to the expression level of GAPDH and presented as expression levels relative to those of nontreated MJD78 cells. Data are presented as the means ± SDs of more than three independent experiments. * $p < 0.05$.

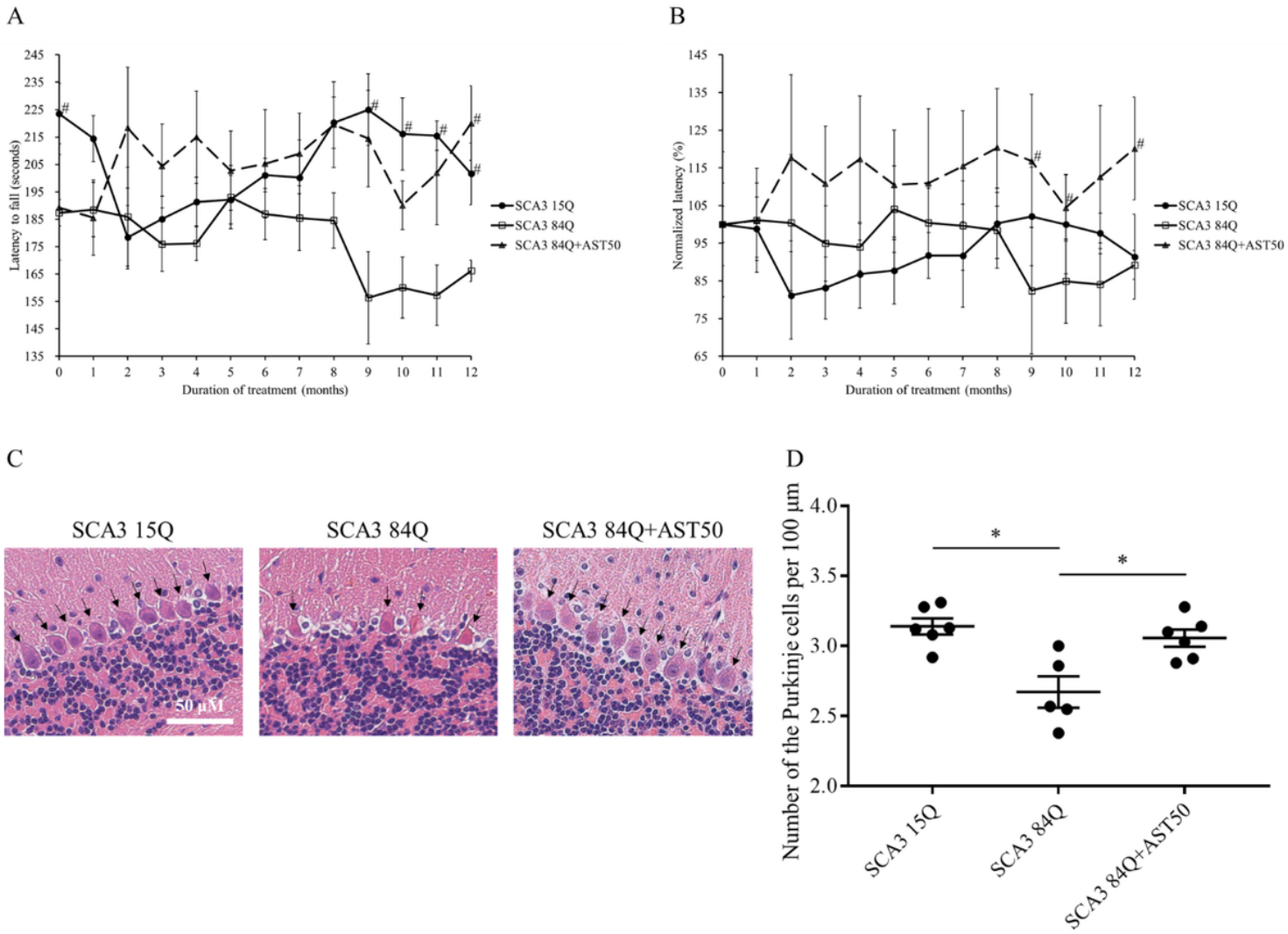

Figure 5

Motor coordination and histopathological analysis of SCA3 mice. (A) Rotarod tests were initiated prior to AST intervention at the age of 6 months. Latency to fall was recorded once a month for 12 months. (B) Within a given group, the latency to fall at 6 months was normalized to 100%. Data are presented as means ± standard errors of the mean (n = 6 per group). # $p < 0.05$, with SCA3 84Q group being the basis for comparison. (C) H&E staining of the cerebellums of mice. Arrows indicate Purkinje cells. (D) Quantification of average number of Purkinje cells per 100 μM. SCA3 15Q, n = 6; SCA3 84Q, n = 5; SCA3 84Q + AST50, n = 6. Data are presented as means ± standard errors of the mean. * $p < 0.05$.

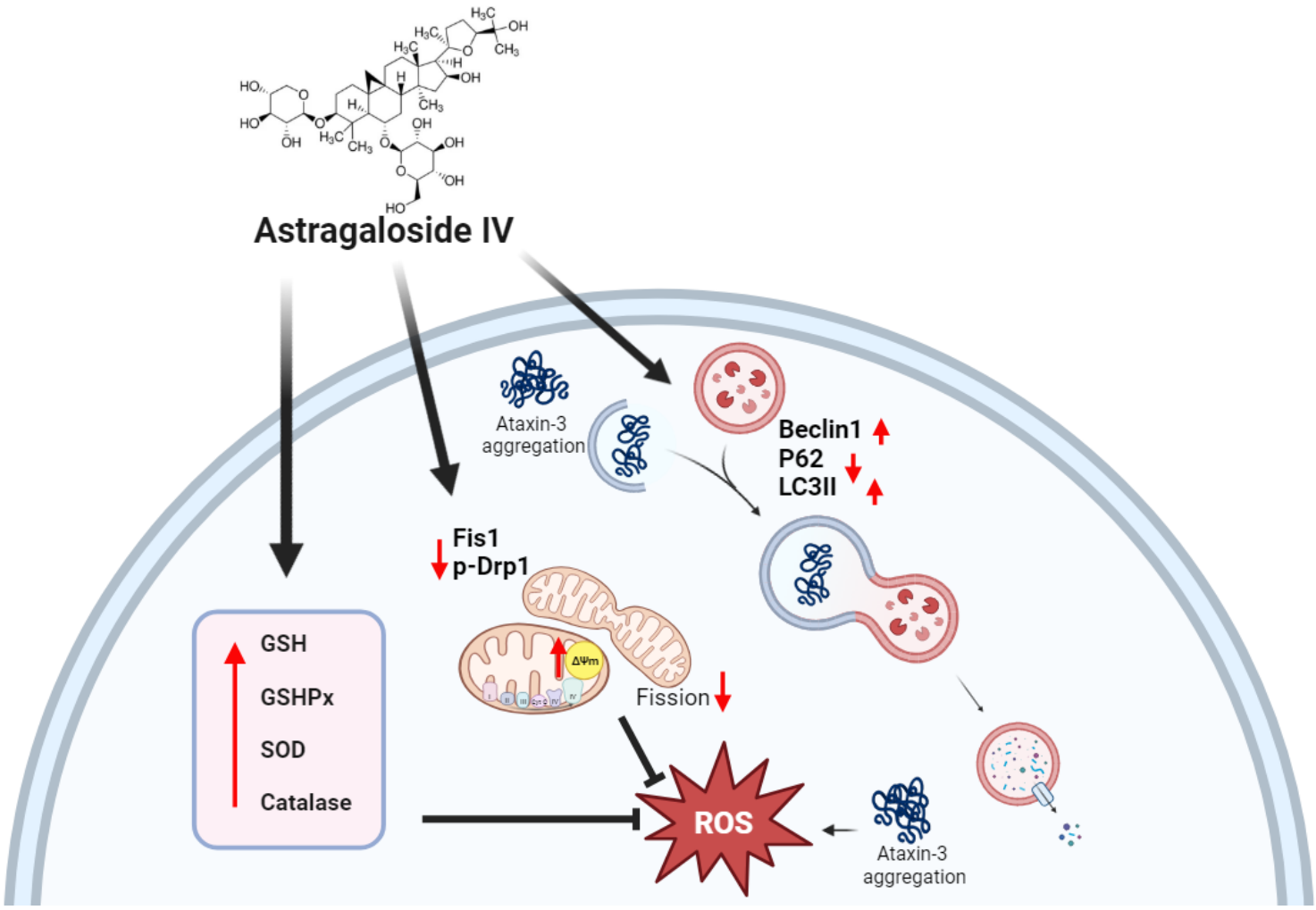

Figure 6

AST intervention in SCA3 Model. AST administration reduced total and mitochondrial ROS, reduced mitochondrial fission, improved mitochondrial function, increased autophagy-related protein expression, increased antioxidant enzyme activity, and reduced intracellular mutant ataxin-3 protein aggregation to achieve therapeutic effectiveness in SCA3 model.

Supplementary Files

This is a list of supplementary files associated with this preprint. Click to download.

- SupplementInformationSI.docx